

# Comparison of Activated Carbon and Physic Seed Hull for the Removal of Malachite Green Dye from Aqueous Solution

Masita Mohammad  · Saikat Maitra ·  
Binay Kanti Dutta

Received: 5 September 2017 / Accepted: 10 January 2018 / Published online: 26 January 2018  
© Springer International Publishing AG, part of Springer Nature 2018

**Abstract** In the present work, the effectiveness of physic seed hull, PSH (*Jatropha curcas* L.), as an alternative low-cost adsorbent for the removal of malachite green (MG) dye from simulated wastewater has been studied. It has been observed that PSH has remarkable adsorption capacity compared to granular activated carbon. The PSH adsorbent was characterized by SEM-EDX, BET, CHNS, zeta potential, and FTIR techniques. The adsorption behaviors such as adsorption kinetics, adsorption dynamics, and adsorption isotherms of PSH for the removal of MG dye from aqueous solution were studied in detail. The kinetic data fitted well with the pseudo second-order kinetic model for MG adsorption. Langmuir isotherm was found to be the model best fitted to describe the adsorption process.

**Keywords** Physic seed hull · Activated carbon · Granular materials · Malachite green · Adsorption · Kinetic · Isothermal

---

M. Mohammad (✉)  
Solar Energy Research Institute (SERI), Universiti Kebangsaan  
Malaysia, 43600 Bangi, Selangor, Malaysia  
e-mail: masita@ukm.edu.my

S. Maitra  
Government College of Engineering & Ceramic Technology, 73  
Abinash Chandra Banerjee Lane, Kolkata 700010, India  
e-mail: maitrasaikat@rediffmail.com

B. K. Dutta  
National Institute of Technology Rourkela, Rourkela, Odisha  
769008, India  
e-mail: binaykdutta@gmail.com

## 1 Introduction

The estimated numbers of different commercial dyes and pigments are around 10,000 at present and their annual productions are over  $7 \times 10^5$  tons globally (Garg et al. 2004). Dyes are extensively used in production of textile, rubber, paper, plastic, cosmetic, etc. (Garg et al. 2003). Synthetic dyes are common water pollutants and often can be found as a trace constituent in industrial wastewater due to their high solubility in water. However, it imparts toxicity to the aquatic life and damages the environment with severe problems which emerge from the discharge of dye-bearing wastewater into natural streams and rivers. It is very difficult to treat wastewater containing dyes since the dyes are resistant to aerobic digestion and are stable to light, heat, and oxidizing agents (Sun and Yang 2003; Ravi Kumar et al. 1998).

Malachite green, also known as aniline green, basic green 4, diamond green B, or Victoria green B [IUPAC name, -(4-dimethylaminophenyl)-phenyl-methyl]-*N,N*-dimethyl-aniline], is a toxic substance. It is frequently used as a dye in industry; used in fish as a topical antiseptic or to treat parasites and fungal, protozoan, and bacterial infections and some other diseases caused by helminths on a wide variety of fish and other aquatic organisms; and as a bacteriological stain. Their contamination in water bodies would harm both animals and human beings due to its carcinogenic and mutagenic effects. The concentration of as low as 0.1 would result in a chromosome division also known as a cytostatic syndrome in experimental fish. The Committee on the Food and Animal Health of the European Commission

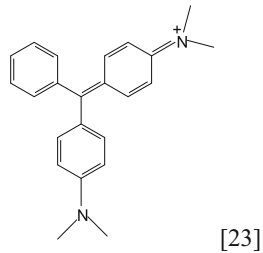


**Fig. 1** Structure of malachite green 125

specified the limitation for total MG and LMG concentration is 0.02 ppm and below (Culp et al. 2002; Srivastava et al. 2004; Cho et al. 2003; Sudova et al. 2007). Due to continued malachite green contamination, FDA blocked the import of several varieties of seafood in June, 2007 (Culp et al. 2002).

Dyes are usually treated by either expensive physical or chemical processes which are not also quite effective in treating the wide range of dye-containing waste (Garg et al. 2003). The efficiency of adsorption for dye removal from wastewater has made it an ultimate alternative compared to other expensive treatment methods (Abdullah et al. 2005). In recent years, adsorption techniques have become popular due to their proven efficiency in the removal of pollutants from effluents. The processes are economically feasible with a high-quality product (McKay 1981; Jumariah et al. 2005). Adsorption techniques also can be used for the removal of different types of coloring materials (Jain et al. 2003; Ho and McKay 2003).

At present, most commercial systems use activated carbon as a sorbent to remove dyes from wastewater, since it has excellent adsorption capacity (McKay 1981; Jumariah et al. 2005). Activated carbon is the most extensively used adsorbent because of their efficiency on organic compound adsorption, but it has some limitation due to its high production and regeneration cost.

**Table 1** Universal buffer mixture

0.2 M Na <sub>2</sub> HPO <sub>4</sub> /mL	0.1 M citric acid/mL	pH
20.55	79.45	3
38.55	61.45	4
51.50	48.50	5
63.15	36.85	6

As a consequence, numerous inexpensive and easily available materials, such as waste biomass, are being studied to remove different dyes from aqueous solutions at different operating conditions for consideration as potential dye adsorbents (Abdullah et al. 2005). Various biomass materials and agricultural by-products have been utilized in the removal of MG from wastewater, such as agroindustry waste, *Phosopsis cineraria* (Garg et al. 2004), marine alga, *Caulerpa racemosa* var. *cylindracea* (Bursali et al. 2009), chitosan bead (Bekci et al. 2008), hen feathers (Mittal 2006), groundnut shell (Malik et al. 2007), carbon prepared from *Arundo donax* root (Zhang et al. 2008), bentonite (Bulut et al. 2008), gelatin-grafted granular composite hydrogel (Zheng et al. 2015), and durian seed-based activated carbon (Mohd Azmier Ahmad et al. 2014).

In this research, the possibility of the use of an industrial agrowaste material, physic seed hull (PSH), for the removal of malachite green dye from aqueous solution has been investigated and its performance was evaluated against that of commercially available granular activated carbon (GAC).

**Table 2** Characteristic of the PSH

Parameter	Value
Sulfur (%)	0.095
Magnesium (%)	0.363
Potassium (%)	1.020
Calcium (%)	1.220
Nitrogen (%)	1.625
Hydrogen (%)	5.785
Carbon (%)	36.623
Oxygen (%)	49.501
Ash (%)	3.768
pH	7.590
pH <sub>pzc</sub>	2.600
Moisture (%)	8.973
Size distribution (mm)	0.15–1.18
Specific surface area (multipoint BET-N <sub>2</sub> ) (m <sup>2</sup> /g)	614.01
External surface area (t-method) (m <sup>2</sup> /g)	89.11
Internal surface area (t-method) (m <sup>2</sup> /g)	524.9
Average pore diameter (Å)	30.760
Total pore volume (cm <sup>3</sup> /g)	0.4722

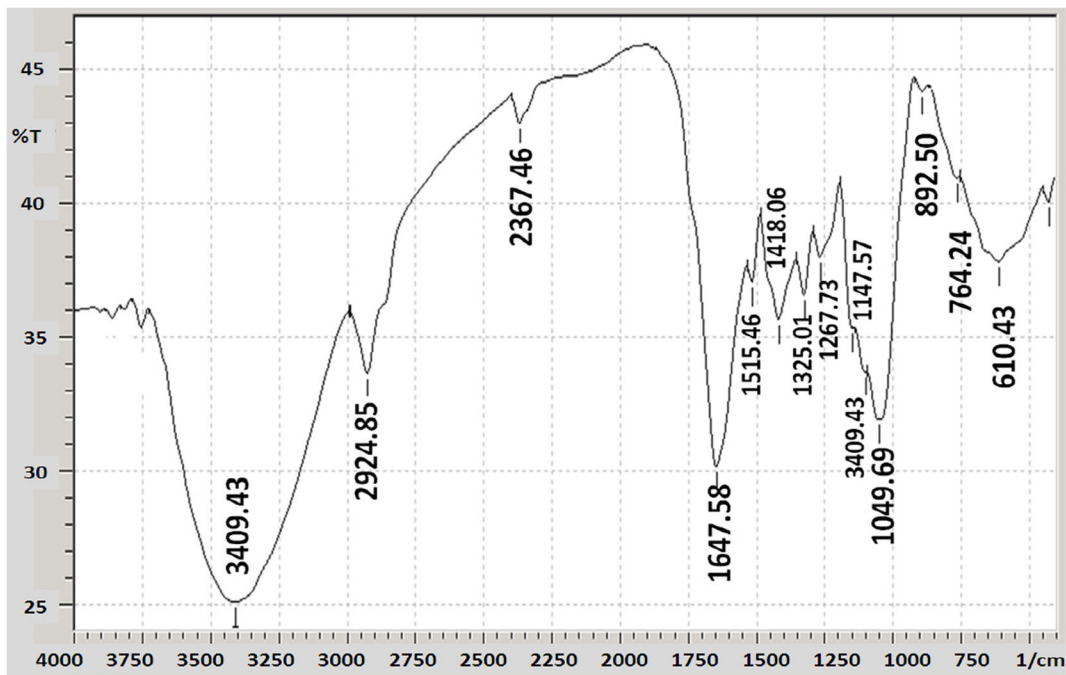


Fig. 2 FT-IR spectrum of PSH

## 2 Methodology

### 2.1 Adsorbents

The PSH sample was collected from Bota, Perak of Malaysia. It was repeatedly washed with water to remove adhering dirt and soluble components. It was then oven-dried at 85 °C until constant weight. The washed and dried material was crushed and sieved using laboratory sieve to obtain a 600- $\mu\text{m}$  size. A similar

procedure was utilized to commercial activated carbon derived from wood (Merck, German).

The PSH and GAC were characterized by Fourier transform infrared (FTIR) spectroscopy, (Spectrum 2000 Explorer; Perkin Elmer Cetus Instruments, Norwalk, CT, USA) to analyze the organic functional groups in the adsorbent. The surface morphologies of PSH and GAC were examined with a field emission scanning electron microscope, SEM-EDX (Leo Supra 50 VP, Germany), with gold-coated samples. Elemental

Fig. 3 Nitrogen adsorption-desorption curves of PSH

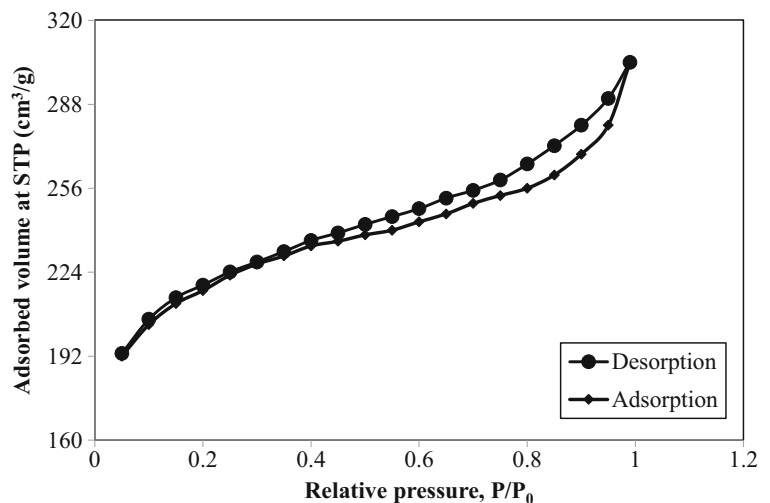
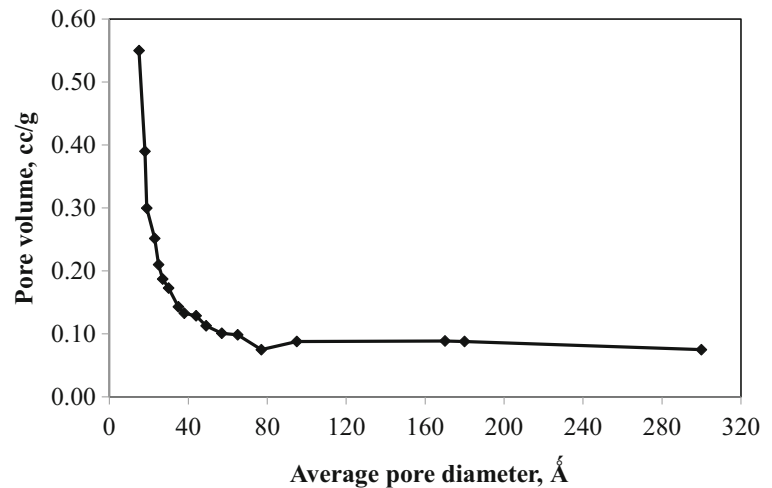


**Fig. 4** Pore size distribution of PSH



composition in terms of C-H-N-S was measured using CHNS analyzer (CHNS 932, LECO, USA). The surface composition of the sorbent was determined by an energy-dispersive X-ray fluorescence (XRF Bruker S4 Pioneer, USA) analysis.

The specific surface area and pore size of PSH and GAC were measured using the BET method by  $N_2$  adsorption isotherm at 77 K using a Quantachrome Autosorb Automated Gas Sorption Instrument, UK. BET method and Barrett–Joyner–Halenda (BJH) methods were used to calculate the surface area and the pore size distribution of PSH and GAC. Total volume of pores was calculated at a relative pressure ( $P/P_0$ ) of 0.99. The zeta potential of PSH was measured using Malvern Zetasizer Nano ZS potentiometer (Malvern Instruments, UK) to assess the surface charge of PSH.

The particle size range was measured using Malvern particle size analyzer (model Master Seizer 2000, UK).

## 2.2 Chemicals

The Malachite green dye [C.I. = 42,000, chemical formula =  $C_{23}H_{26}N_2Cl$ , molecular weight 329.50;  $\lambda_{max} = 617$  nm (reported)] was obtained from Bendosen Laboratory Chemical, UK. The dye used was an analytical grade chemical without further purification. Stock solutions of dye with concentrations ranging from 10 to 50 ppm were prepared by dissolving the dye in deionized water. The pH was adjusted using universal buffer mixture (0.2 M  $NH_2HPO_4$ /mL and 0.1 M citric acid/mL) to avoid the changes on pH due to the presence of functional groups at the surface

**Fig. 5** The zeta potential curves as a function of pH for PSH

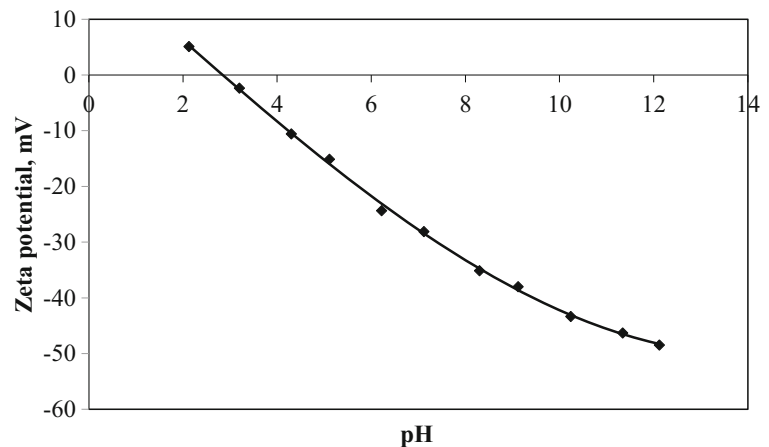
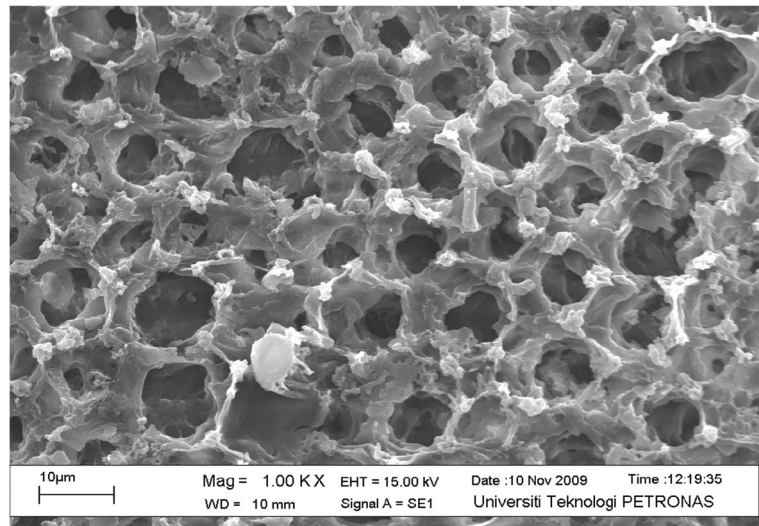


**Fig. 6** SEM image of PSH (600  $\mu$ ,  $\times 1000$ )



of PSH (Table 1) (Medham et al. 2000). The concentrations of dyes were measured using UV-VIS spectrophotometer (HACH UV-VIS Spectrophotometer DR 5000, USA). The pH was measured by Orion pH meter. The chemical structure of malachite green is as shown in Fig. 1 (Christie 2001).

### 2.3 Adsorption Experiment

The equilibrium and batch adsorption experiments were carried out by shaking 0.4 g of the sorbent with 100 mL of the solution containing the desired concentrations of the MG dye solution. The mixed

solution and the sorbent were agitated in a closed polyethylene bottle for 7 h using a laboratory shaker at 160 rpm (Thermolyne Big Bill Digital Orbital Shaker, M73620-26, USA). All measurements were conducted at room temperature ( $24 \pm 1$  °C) and pH 6. Then, the suspensions were filtered through a 0.45- $\mu$ m syringe filter. The filtrate was analyzed using UV-VIS spectrophotometer (HACH UV-VIS Spectrophotometer DR 5000, USA). The experiments were carried out by varying the initial dye concentrations and type of adsorbent for PSH and GAC as comparison. Adsorption rates were measured according to the

**Fig. 7** SEM image of GAC (600  $\mu$ ,  $\times 1000$ )

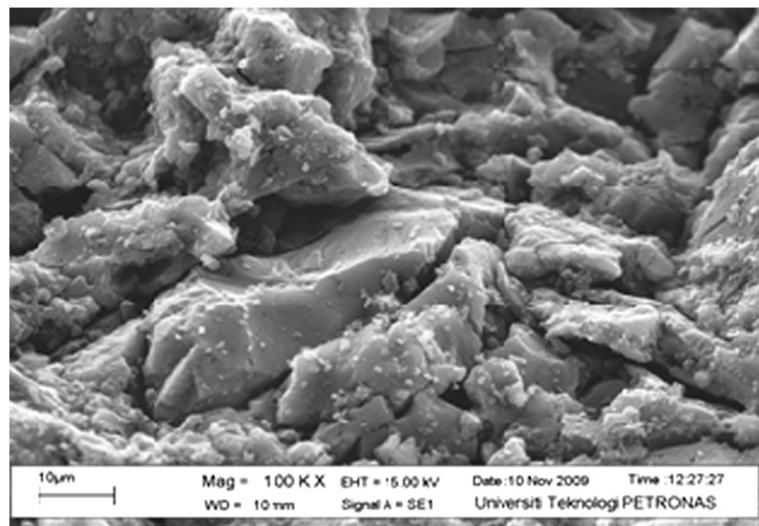
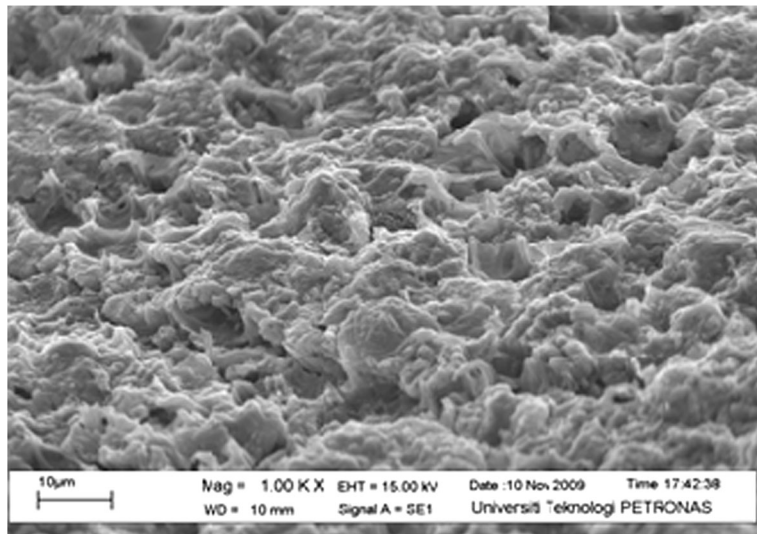




**Fig. 8** SEM image of PSH after adsorption (600  $\mu$ ,  $\times 1000$ )



predefined procedure with dye concentrations ranging from 10 to 50 ppm.

### 3 Results and Discussions

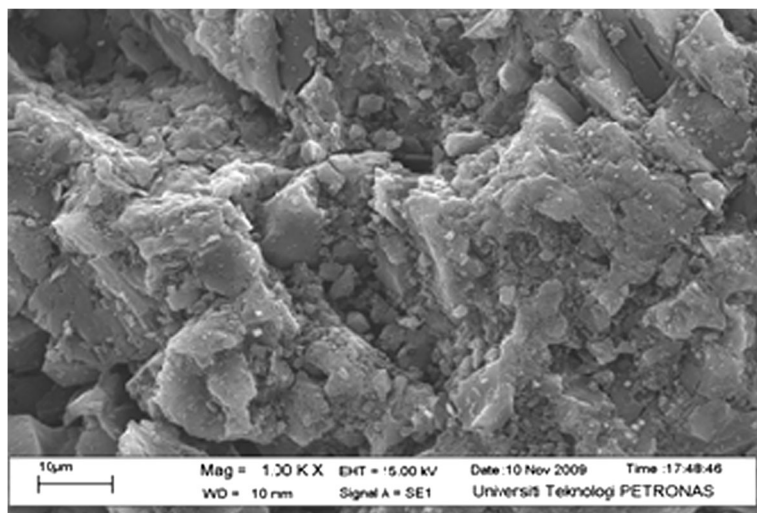
#### 3.1 Characteristic of Adsorbent

Table 2 represents the physical characteristics together with the elemental distribution of the PSH. From the table, it shows that the specific surface area of PSH (614  $\text{m}^2/\text{g}$ ) is quite high compared to that of the commercial activated carbon (589.87  $\text{m}^2/\text{g}$ ). Rao et al. (2006) obtained 521  $\text{m}^2/\text{g}$  specific surface areas for

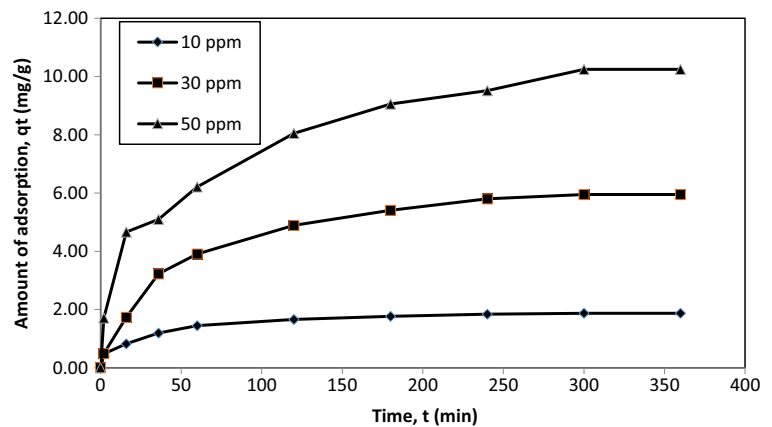
activated carbon derived from *Ceiba pentandra* hulls (Ramesh et al. 2006).

The FTIR spectrum, the nitrogen adsorption-desorption curves, pore size distribution, zeta potential curves of PSH, and SEM photographs of the PSH and GAC are shown in Figs. 2, 3, 4, 5, 6, 7, 8, and 9. From the FTIR spectrum, the absorption at 3410/cm indicates the presence of OH group, which may be attributed to the adsorbed water on the carbon (Ramesh et al. 2006; Vinke et al. 1994; Chen et al. 2002). The existence of hydroxyl groups on adsorbent surface shows the availability of negatively charged sites which may develop the attraction between dye and adsorption surface (Schnoor 1996; Husseien et al. 2007). In this case, the

**Fig. 9** SEM image of GAC after adsorption (600  $\mu$ ,  $\times 1000$ )



**Fig. 10** Effect of contact time on MG adsorption by PSH with different initial dye concentrations (pH 6, PSH dosage 4 g/L, temp. 24 °C and shaker speed 160 rpm, size 0.6 mm)



PSH acted as a negative surface that attracted the cationic dye (MG). The bands appearing at 1648/cm are ascribed to the formation of oxygen functional groups like a highly conjugated C=O stretching in carboxylic groups and carboxylate moieties as well as strong intensity of amides. The peaks at 1049 to 1648/cm indicate the presence of C-H and S=O groups, respectively. The C=O and S=O functional groups show strong coordination with cationic metal ions (probably, they have similar affinity towards cationic dyes) (Ramesh et al. 2006; Pearson 1988; Krishnan and Anirudhan 2003). Based on the Pearson theory of acid-base reaction, hard acids prefer to interact with hard bases and soft acids with soft bases. In this case, positively charged cationic dye (MG) is a soft acid which likely favors the surface hydroxyl group of PSH acting as a soft base. In addition to hydroxyl group, carboxyl and sulphonyl groups

contained in PSH are also responsible for the sorption of cationic substances akin to MG (Pearson 1988; Krishnan and Anirudhan 2003).

The presence of the band in the region of 3409–1648/cm indicates the existence of aromatic compounds. Amino groups act as a base because ammonia can pick up a hydrogen ion ( $H^+$ ) from the solution. The typical N-H absorption pattern corresponding to amine group which stretches at 3409/cm is an indication of the increase in water pH when the PSH was soaked in distilled water (Marcilla et al. 2007). The nitrogen adsorption-desorption curves of PSH is illustrated in Fig. 3. The adsorbed volume increased with an increase in  $P/P_0$ , indicating a wider pore size distribution in the adsorbent PSH. This porous adsorbent can be classified as type II isotherm associated with stronger fluid-solid interactions (Barton et al. 1999). Figure 4 shows the pore size

**Fig. 11** Effect of contact time on MG adsorption by GAC with different initial dye concentrations (pH 6, GAC dosage 4 g/L, temp. 24 °C and shaker speed 160 rpm, size 0.6 mm)

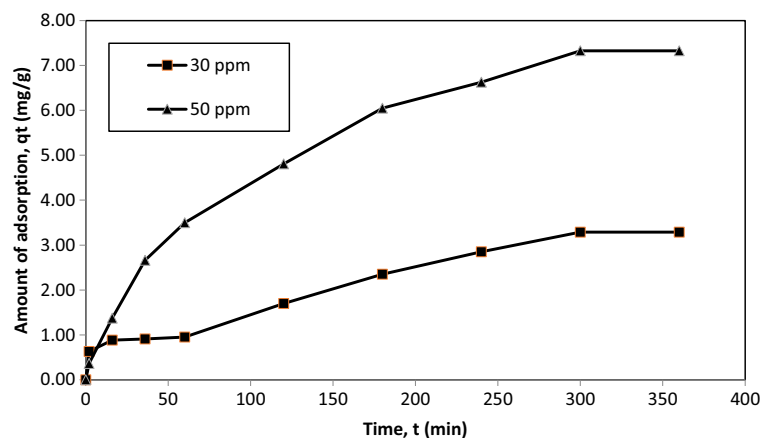
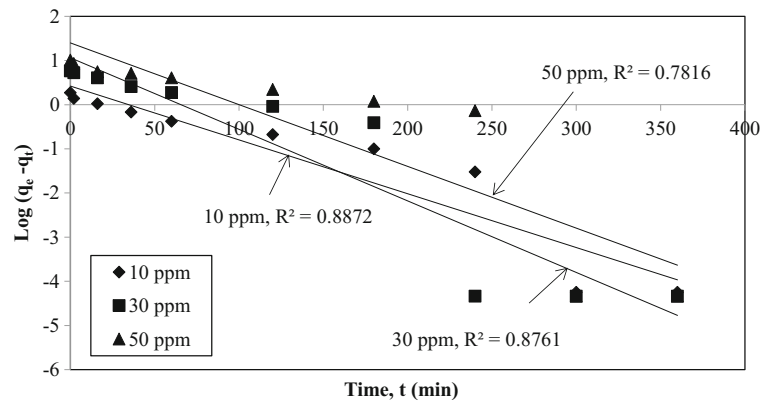


**Fig. 12** Pseudo first-order kinetic model for MG adsorption by PSH at different initial dye concentrations (dosage 4 g/L, initial solution pH 6, shaker speed 160 rpm, temp. 24 °C, particle size 600  $\mu$ )



distributions of PSH. It appears that PSH contains both micropores and mesopores. From the nature of porosity, the adsorption process can be considered as a mesopore-dominated capillary condensation phenomenon. The strong interaction between adsorbate molecules and pore walls further controls the filling of micropores during the adsorption process (Barton et al. 1999).

Figure 5 shows the variation of zeta potential of PSH as a function of pH. Zeta potential is the manifestation of surface charge density of the adsorbent. Surface charge density has a significant effect on cation adsorption on PSH. The pH at the point of zero charge  $pH_{pzc}$  of PSH is 2.6, while  $pH_{pzc}$  for GAC derived from wood reported by Rangel-Mandez and Streat (2001) is 2.29. The  $pH_{pzc}$  value is the point at which surface functional groups do not contribute to the pH of the solution. Above this pH value, the surface charge becomes negative and the adsorbent will adsorb the cations (Abia and Asuquo 2006).

Scanning electron microscopic photographs of PSH shown in Fig. 6 reveal the surface texture and porosity of the sample. The availability of pores and internal

surface is requisite for an effective adsorbent. It is clear that PSH has considerable numbers of pores and there is a good possibility for dyes to be trapped and adsorbed into these pores. According to the results obtained, PSH could be employed as a low-cost adsorbent and could be considered as an alternative adsorbent for the adsorption of MG. The SEM image of GAC is shown in Fig. 7 as a comparison and it shows smaller number and size of pores compared to PSH pores. Figures 8 and 9 show the SEM images of PSH and GAC with occupied pores after the adsorption of MG.

### 3.2 Comparison Studies

#### 3.2.1 Adsorption Kinetics at Different Initial Concentrations

The effect of initial concentration on the adsorption of MG from the aqueous solutions using PSH and GAC was studied. The experiments were carried out at a fixed adsorbent dose (0.4 g/100 mL) in the test solution and at

**Fig. 13** Pseudo first-order kinetic model for MG adsorption by GAC at different initial dye concentrations (dosage 4 g/L, initial solution pH 6, shaker speed 160 rpm, temp. 24 °C, particle size 600  $\mu$ )

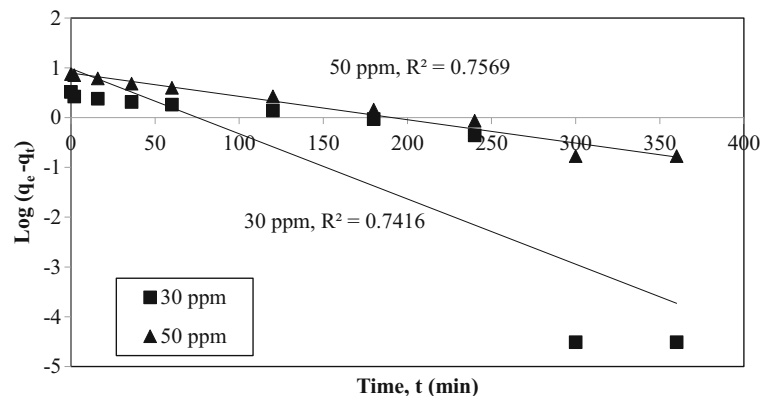
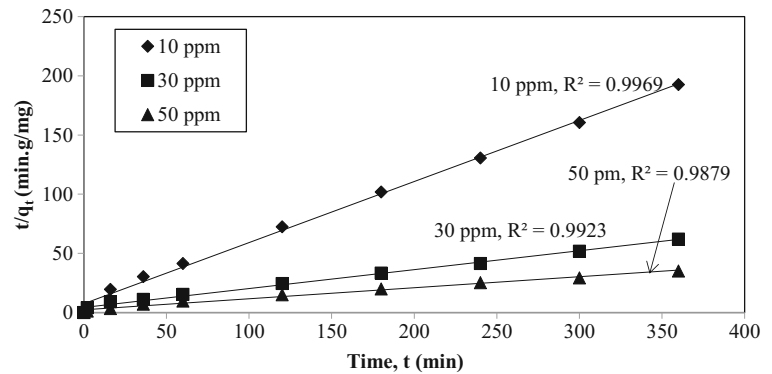




**Fig. 14** Pseudo second-order kinetic model for MG adsorption by PSH at different initial dye concentrations (dosage 4 g/L, initial solution pH 6, shaker speed 160 rpm, temp. 24 °C, particle size 0.6 mm)



24 °C temperature and pH 6 for different time intervals (2–360 min). The adsorption capacity of PSH and GAC increased with the increase in initial dye concentration in the solution (Figs. 10 and 11). The equilibrium capacity for PSH was 1.9384, 6.4103, and 10.7296 mg/g as the MG concentration in the test solution was increased from 10, 30, and 50 mg/L, respectively. Similarly, adsorption capacity for GAC was increased from 3.5361 to 8.3963 mg/g as the dye concentration in the test solution was increased from 30 to 50 mg/L, respectively.

From the results, it was shown that the GAC took more time to reach equilibrium with lesser adsorption capacity, while PSH gathered higher adsorption capacity with lesser time spent to reach equilibrium. Both the time profiles for adsorption of MG are single and smooth and are continuous curves leading to saturation. It suggested the potential monolayer

coverage of dye on the surface of the adsorbent (Ho et al. 1996) and this is also proved by the good fit of the adsorption data with the Langmuir model. Again, PAH and GAC have macro- and micropores. For the adsorption process, a three-step process is involved: initially, the dye molecules have to first encounter the boundary layer effect and then they have to diffuse from the boundary layer film onto the adsorbent surface. After a relatively longer contact time, they diffuse into the porous structure of the adsorbent; and finally, the equilibrium is reached when no further adsorption is taking place (Malik 2003; Jain 2001).

### 3.2.2 Adsorption Dynamics

The  $R^2$  value from the Lagergren pseudo first-order plot (Figs. 12 and 13) has been compared with the  $R^2$  value from the pseudo second-order plot (Figs. 14 and 15) for

**Fig. 15** Pseudo second-order kinetic model for MG adsorption by GAC at different initial dye concentrations (dosage 4 g/L, initial solution pH 6, shaker speed 160 rpm, temp. 24 °C, particle size 0.6 mm)

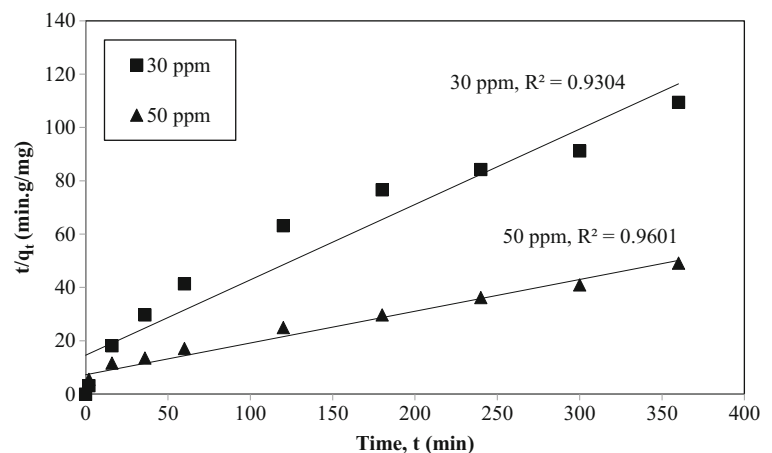


**Table 3** Kinetic parameters for the adsorption of MG on PSH and GAC

System parameter			
$K_2$ (g/mg min)	$q_e$ (mg/g)	$h$ (mg/g min)	$R^2$
Effect of initial concentration of MG using PSH			
10 ppm (mg/L)			
0.0355	1.9384	0.1333	0.9969
30 ppm (mg/L)			
0.0054	6.2617	0.2324	0.9923
50 ppm (mg/L)			
0.0037	10.7296	0.4303	0.9879
Effect of initial concentration of MG using GAC			
30 ppm (mg/L)			
0.0047	3.5361	0.0688	0.9304
50 ppm (mg/L)			
0.0019	8.3963	0.1381	0.9601

the adsorption of MG on PSH and GAC (Eq. 2) (Lagergren and Svenska 1898). From the  $R^2$  values for both plots, it is apparent that the adsorption dynamic fitted well with pseudo second-order kinetics model as the regression coefficient is higher or closer to 1. A plot between  $t/q_t$  versus  $t$  gives the value of the rate constants  $K_2$  (g/mg h), equilibrium capacity  $q_e$  (mg/g), and initial sorption rate  $h$ , and all the adsorption kinetic parameters were tabulated in Table 3 (Eqs. 3, 4, 5). This further suggests the assumption behind the pseudo second-order model that chemisorption is the rate-controlling step here. Also from Table 3, it is clear that the initial sorption rate  $h$  and the adsorption capacity increased with the increase in dye concentration. Ho's pseudo second-order model has been applied extensively for the adsorption of metal ions, dyes, herbicides, oils, and organic substances from aqueous systems (Chen et al. 2002; Adamson 1967).

### 3.2.3 Adsorption Isotherms

The Langmuir, Freundlich, and Dubinin–Radushkevich isotherms were utilized to analyze the equilibrium isotherms in this study. Langmuir isotherm assumes that the coverage of adsorbate over a homogenous adsorbent surface basically is a monolayer (Langmuir 1918). A basic assumption is that sorption takes place at specific homogenous sites within the adsorbent. Once a dye

molecule occupies a site, no further adsorption can take place at that site. Furthermore, there is no interaction between the adsorbate molecules and the sorption becomes localized in a monolayer. The Langmuir adsorption isotherm has been successfully used to explain the adsorption of dyes from aqueous solutions (Garg et al. 2004; Garg et al. 2003; Sun and Yang 2003; Abdullah et al. 2005; Jumasih et al. 2005; Jain et al. 2003; Ho and McKay 1978; Freundlich 1926; Janoš and Šmídová 2005). The equilibrium data were better fitted to Langmuir isotherm and the resulting constants together with the  $R^2$  value are as listed in Table 4 (refer to Eq. 6).

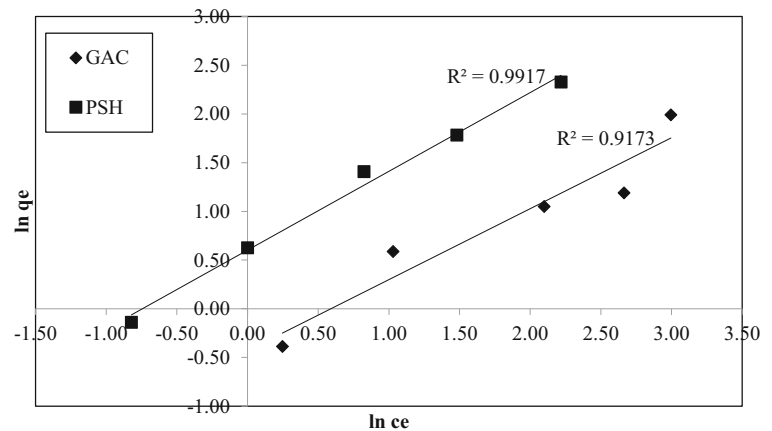
The Freundlich isotherm is an empirical equation with the assumption that the adsorption process takes place on heterogeneous surfaces with interaction between adsorbed molecules. The non-uniform distribution of adsorption over the surface and the adsorption capacity are related to the concentration of MG dye at equilibrium (Freundlich 1926). By referring to the Freundlich isotherm model, Eq. 8,  $K_f$  (mg/g (L/mg)  $1/n$ ) is roughly an indicator of the adsorption capacity and  $1/n$  is the adsorption intensity. The magnitude of the exponent,  $1/n$ , gives an indication of the favorable behavior of adsorption. Values of  $n > 1$  represent favorable adsorption condition (Horsfall and Spiff 2005; Treybal 1968). Table 3 shows the values of  $K_f$ ,  $n$ , and the linear regression correlation ( $R$  (Garg et al. 2003)) for Freundlich model.

Figures 16 and 17 show that Langmuir isotherm fits the data better than Freundlich for both the adsorbents. This is also confirmed by the high value of  $R^2$  in the case of Langmuir (0.9995) compared to Freundlich (0.9917) for PSH, and that of Langmuir (0.9679) compared to Freundlich (0.9173) for GAC. This indicates that the adsorption of MG on PSH and GAC occurs as monolayer

**Table 4** Isotherm parameters for the adsorption of MG on PSH and GAC

Parameters	PSH	GAC
Langmuir, $K_a$	0.0945	0.0572
$q_m$	21.7865	10.3413
$R^2$	0.9995	0.9679
$R_L$	0.1747	1.2591
Freundlich, $n$	1.2367	1.3729
$K_f$	0.5477	1.2367
$R_2$	0.9917	0.9173

**Fig. 16** Freundlich plots for MG adsorption on PSH and GAC (initial solution pH 6, amount of adsorbent 4 g/L, temp. 24 °C and shaker speed 160 rpm, particle size 0.6 mm)



adsorption on a homogenous surface. Table 3 indicates that the computed maximum monolayer adsorption capacity ( $q_m$ ) of PSH for MG was relatively large, which was 21.7865 mg/g compared to that of GAC which was 10.3413 mg/g.

The essential characteristics of the Langmuir isotherm can be expressed in terms of a dimensionless constant separation factor  $R_L$  that is given by Eq. 7 (Hall et al. 1966). The  $R_L$  value for the adsorption of MG onto PSH is 0.1747 and GAC is 1.2591. The  $R_L$  values between 0 and 1 indicate favorable adsorption. Figure 18 shows the  $R_L$  values obtained and the values are decreased with the increment of initial dye concentration. This indicated that the adsorption is a favorable process and at high initial MG concentrations, the adsorption is almost irreversible or more favorable.

#### 4 Discussions and Conclusion

The removal of malachite green from simulated wastewater using physic seed hull and granular activated carbon has been investigated under different experimental conditions in batch mode. The PSH is a locally available low-cost material and can be used as an alternative adsorbent for the removal of MG from aqueous solutions without any pretreatment. The adsorption of MG is dependent on adsorbent surface characteristics, time contact, and dye concentration in the wastewater. Maximum dye was removed within 3 h of the kinetic process. The adsorption dynamic fitted well with Lagergren pseudo second-order kinetics model, while the adsorption isotherm fitted better with Langmuir model compared to Freundlich model. The results show remarkable capacity of PSH for MG adsorption

**Fig. 17** Langmuir plots for MG adsorption on PSH and GAC (initial solution pH 6, amount of adsorbent 4 g/L, temp. 24 °C and shaker speed 160 rpm, particle size 600 mm)

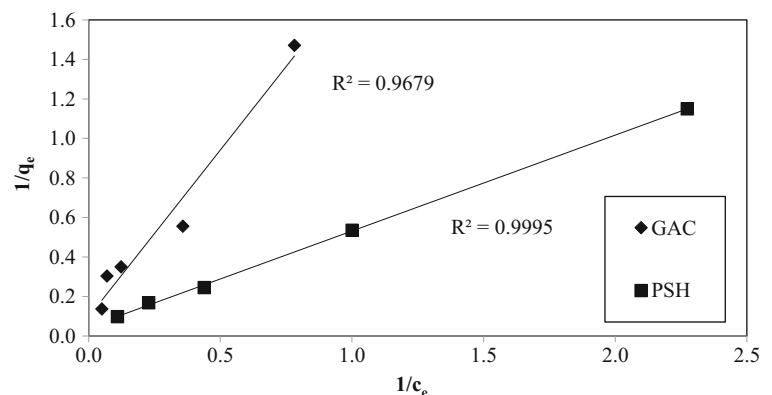
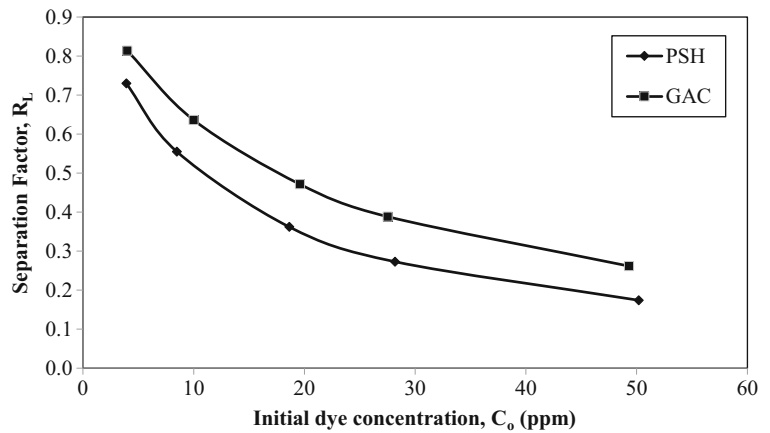


**Fig. 18** Separation factor from Langmuir equation



compared to GAC. Due to some limitations such as faster degradation of the PSH, the PSH will be considered for physical activation and, theoretically, with additional chemical activation it would generate more pores and get higher adsorption capacity due to its remarkable capacity. The data is valuable for designing and fabricating an economical treatment process using batched or stirred-tank flow reactors for the removal of MG from dilute industrial effluents.

**Acknowledgments** The authors greatly acknowledge the financial support FRGS/1/2014/TK04/UKM/03/2 and GGPM-2014-027 from CRIM (Centre of Research and Instrument Management, UKM and KPT (Kementerian Pengajian Tinggi), Malaysia.

**Author Contributions** M.M. performed the experimental works, analyzed the data, and wrote the manuscript, S. M. designed the experiment, and B.K.D. performed the technical check and modeling.

**Conflict of Interest** The authors declare that they have no conflict of interest.

**Appendix**

The dye concentration retained in the adsorbent phase:

$$q_t = \frac{(C_0 - C_t) V}{m} \tag{1}$$

The Lagergren pseudo first-order model (Lagergren and Svenska 1898):

$$\log(q_e - q_t) = \log q_e - \frac{K_1}{2.303} t \tag{2}$$

Pseudo second-order model (Jain 2001; Ho and Mckay 1998):

$$\frac{dq}{dt} = K_2 (q_e - q_t)^2 \tag{3}$$

Integrating and applying boundary conditions  $t = 0$  to  $t = t$  and  $q = 0$  to  $q = q_t$  gives:

$$\frac{t}{q_t} = \frac{1}{K_2 q_e^2} + \frac{1}{q_e} t \tag{4}$$

A plot between  $t/q_t$  versus  $t$  allows the value of the constants  $K_2$  (g/mg h) and  $q_e$  (mg/g) to be calculated. The constant  $K_2$  is used to calculate the initial sorption rate  $h$ , at  $t \rightarrow 0$ , as follows:

$$h = K_2 q_e^2 \tag{5}$$

The linearized form of Langmuir isotherm (Langmuir 1918):

$$\frac{1}{q_e} = \left( \frac{1}{K_a q_m} \right) \frac{1}{C_e} + \frac{1}{q_m} \tag{6}$$

Dimensionless constant separation factor  $R_L$  (Hall et al. 1966):

$$R_L = \frac{1}{1 + bC_0} \tag{7}$$

The value of  $R_L$  indicates  $R_L = 1$ , favorable ( $0 < R_L < 1$ ) or irreversible ( $R_L = 0$ ).

The linearized form of Freundlich adsorption isotherm (Adamson 1967; Freundlich 1926):

$$\ln q_e = \ln K_f + \frac{1}{n} (\ln C_e) \tag{8}$$

## Notation

A	Area, m <sup>2</sup>
V	Volume, m <sup>3</sup>
R <sub>L</sub>	Separation factor
C <sub>0</sub>	Initial concentration, mg/L
C <sub>e</sub>	Equilibrium concentration, mg/L
h	Initial adsorption rate
k <sub>1</sub>	Rate constant for first-order model, per minute
k <sub>2</sub>	Rate constant for second-order model, g/mg h
k <sub>a</sub>	Rate constant for Langmuir, mg/g
k <sub>f</sub>	Rate constant for Freundlich
n	adsorption intensity for Freundlich
b	Langmuir constant, L/mg
q <sub>e</sub>	Adsorbed amount at equilibrium, mg/g
q <sub>t</sub>	Adsorbed amount at t time, mg/g
q <sub>m</sub>	Adsorbed amount at maximum monolayer, mg/g
t	Time, min
t <sub>1/2</sub>	Half-time for adsorption, min
m	Mass, g
R <sup>2</sup>	Regression correlation coefficient
T	Temperature, °C

## Greek letters

Å	Angstrom
λ <sub>max</sub>	Maximum wavelength, nm

## References

- Abdullah, A. G. L., Mohd Salleh, M. A., Siti Mazlina, M. K., Megat Mohd Noor, M. J., Osman, M. R., Wagiran, R., & Sobri, S. (2005). Azo dye removal by adsorption using waste biomass: sugarcane bagasse. *International Journal of Engineering and Technology*, 2(1), 8–13.
- Abia, A. A., & Asuquo, E. D. (2006). Lead (ii) and nickel (ii) adsorption kinetics from aqueous metal solutions using chemically modified and unmodified agricultural adsorbents. *African Journal of Biotechnology*, 5(16), 1475–1482.
- Adamson, A. W. (1967). *Physical chemistry of surfaces* (2nd ed.). New York: Interscience Publishers Inc..
- Barton, T. J., Bull, L. M., Klemperer, W. G., Loy, D. A., McEnaney, B., Misono, M., Monson, P. A., Pez, G., Scherer, G. W., Vartuli, J. C., & Yaghir, O. M. (1999). Tailored porous materials. *Chemistry of Materials*, 11, 2633–2656.
- Bekci, Z., Ozveri, C., Seki, Y., & Yurdakoc, K. (2008). Sorption of malachite green on chitosan bead. *Journal of Hazardous Materials*, 154, 254–261.
- Bulut, E., Ozacar, M., & Sengil, I. A. (2008). Adsorption of malachite green onto bentonite: Equilibrium and kinetic studies and process design. *Microporous and Mesoporous Materials*, 115, 234–246.
- Bursali, E. A., Cavas, L., Seki, Y., Bozkurt, S. S., & Yurdakoc, M. (2009). Sorption of boron by invasive marine seaweed: *Caulerpa racemosa* var. *cylindracea*. *Chemical Engineering Journal*, 150, 385390. <https://doi.org/10.1016/j.cej.2009.01.016>
- Chen, X., Jeyaseelan, S., & Graham, N. (2002). Physical and chemical properties study of the activated carbon made from sewage sludge. *Waste Management*, 22, 755–760.
- Cho, B. P., Yang, T., Blankenship, L. R., Moody, J. D., Churchwell, M., Beland, F. A., & Culp, S. J. (2003). Synthesis and characterization of N-demethylated metabolites of malachite green and leucomalachite green. *Chemical Research in Toxicology*, 16(3), 285–294. <https://doi.org/10.1021/tx0256679>
- Christie, R. M. (2001). *Colour chemistry* (p. 205). U.K.: The Royal Society of Chemistry.
- Culp, S. J., Beland, F. A., Heflich, R. H., Benson, R. W., Blankenship, L. R., Webb, P. J., Mellick, P. W., Trotter, R. W., Shelton, S. D., Greenlees, K. J., & Manjanatha, M. G. (2002). Mutagenicity and carcinogenicity in relation to DNA adduct formation in rats fed leucomalachite green. *Mutation Research*, 506-507, 55–63. [https://doi.org/10.1016/S0027-5107\(02\)00152-5](https://doi.org/10.1016/S0027-5107(02)00152-5)
- Freundlich, H. (1926). *Colloid and capillary chemistry*. London: Methuen.
- Garg, V. K., Gupta, R., Vadar, A. B., & Kumar, R. (2003). Dye removal from aqueous solution by adsorption on treated sawdust. *Bioresource Technology*, 89, 121–124.
- Garg, V. K., Kumar, R., & Gupta, R. (2004). Removal of malachite green dye from aqueous solution by adsorption using agroindustries waste: a case study of *Phosopis ceneraria*. *Dyes and Pigments*, 62, 1–10.
- Hall, K. R., Eagleton, L. C., Acrivos, A., & Vermeulen, T. (1966). Pore- and solid-diffusion kinetics in fixed-bed adsorption under constant-pattern conditions. *I & EC Fundam.*, 5, 212–223.
- Ho, Y. S., & McKay, G. (1978). Sorption of dye from aqueous solution by peat. *Chemical Engineering Journal*, 70, 115–124.
- Ho, Y. S., & McKay, G. (2003). Sorption of dyes and copper ions onto biosorbents. *Process Biochemistry*, 38, 1047–1061.
- Ho, Y.S. and McKay, J.C., 1998. Kinetic models for the sorption of dye from aqueous solution by wood. *Trans IChemE*, Vol 76, Part B.
- Ho, Y. S., Wase, D. A. J., & Forster, C. F. (1996). Kinetic studies of competitive heavy metal adsorption by sphagnum moss peat. *Environmental Technology*, 17, 71–77.
- Horsfall, M. J., & Spiff, A. I. (2005). Equilibrium sorption study of Al<sup>3+</sup>, Co<sup>2+</sup> and Ag<sup>+</sup> in aqueous solutions by fluted pumpkin (Telfairia Occidentalis Hook f.) *Waste Biomass. Acta Chim*, 52, 174–181.
- Hussein, M., Amer, A. A., El-Maghraby, A., & Taha, N. A. (2007). Utilization of barley straw as a source of an activated carbon for removal of methylene blue from aqueous solution. *Journal of Applied Sciences Research*, 3(11), 1352–1358.
- Jain, A. K., Gupta, V. K., Bhatnagar, A., & Suhas. (2003). Utilization of industrial waste products as adsorbents



- for the removal of dyes. *Journal of Hazardous Materials, B101*, 31–42.
- Jain, C. K. (2001). Adsorption of zinc onto bed sediments of the river Ganga; adsorption models and kinetics. *Hydrol. Sci. J. des Sci. Hydrologiques.*, 46(3), 419–434.
- Janoš, P., & Šmídová, V. (2005). Effects of surfactants on the adsorptive removal of basic dyes from water using an organomineral sorbent—iron humate. *Journal of Colloid and Interface Science*, 291, 19–27.
- Jumasiah, A., Chuah, T. G., Gimbon, J., Choong, T. S. Y., & Azni, I. (2005). Adsorption of basic dye onto palm kernel shell activated carbon: sorption equilibrium and kinetics studies. *Desalination*, 186, 57–64.
- Krishnan, K.A. and Anirudhan, T.S., 2003. Removal of cadmium (II) from aqueous solutions by steam activated sulphurised carbon prepared from sugar-cane bagasse pith: kinetics and equilibrium studies. ISSN 0378-4738 = Water SA Vol. 29 No. 2.
- Lagergren, S., & Svenska, B. K. (1898). Zur theorie der sogenannten adsorption gelöster stoffe. *Veternskapsakad Handlingar*, 24(4), 1–39.
- Langmuir, I. (1918). The adsorption of gases on plane surfaces of glass, mica, and platinum. *Journal of the American Chemical Society; Soc.*, 40, 1361–1403.
- Malik, P. K. (2003). Use of activated carbons prepared from sawdust and rice-husk for adsorption of acid dyes: a case study of acid yellow 36. *Dyes and Pigments*, 56, 239e49.
- Malik, R., Ramteke, D. S., & Wate, S. R. (2007). Adsorption of malachite green on groundnut shell waste based powdered activated carbon. *Waste Management*, 27, 1129–1138.
- Marcilla, A., Beltrán, M. I., & Navarro, R. (2007). Application of TG/FTIR to the study of the regeneration process of HUSY and HZSM5 zeolites. *Journal of Thermal Analysis and Calorimetry*, 87(2), 325–330.
- McKay, G. (1981). Design models for adsorption systems in wastewater treatment. *Journal of Chemical Technology and Biotechnology*, 81(31), 717–731.
- Medham, J., Denny, R.C., Barnes, J.D., Thomas, M., 2000. Vogel's textbook of quantitative chemical analysis (5th. ed.). Harlow, Pearson Education.
- Mittal, A. (2006). Adsorption kinetics of removal of a toxic dye, malachite green, from wastewater by using hen feathers. *Journal of Hazardous Materials*, 133, 196–202.
- Mohd Azmier Ahmad, M. A., Ahmad, N., & Bello, O. S. (2014). Adsorptive removal of malachite green dye using durian seed-based activated carbon. *Water, Air, and Soil Pollution*, 225, 2057.
- Pearson, R. G. (1988). Absolute electronegativity and hardness: application. *Inorganic Chemistry*, 27, 734–738.
- Rao, M. M., Ramesh, A., Rao, G. P. C., & Seshiah, K. (2006). Removal of copper and cadmium from the aqueous solutions by activated carbon derived from *Ceiba pentandra* hulls. *Journal of Hazardous Materials*, 129, 123–129.
- Rangel-mendez, J.R. and Streat, M., 2001. Mercury and cadmium adsorption by conventional and modified granular activated carbon. The American Carbon Society. Carbon Conference Archive 1995–2007, 25.4.
- Ravi Kumar, M. N. V., Sridhari, T. R., Bhavani, K. D., & Dutta, P. K. (1998). Trends in colour removal from textile mill effluents. *Colorage*, 40, 25–34.
- Schnoor, J. L. (1996). *Environmental modeling: fate and transport of pollutants in water, air and soil*. New York: Wiley and Sons INC..
- Srivastava, S., Sinha, R., & Roy, D. (2004). Toxicological effects of malachite green. *Aquatic Toxicology*, 66, 319–329.
- Sudova, E., Machova, J., Svobodova, Z., & Vesely, T. (2007). Negative effects of malachite green and possibilities of its replacement in the treatment of fish eggs and fish: a review. *Veterinary Medicinal*, 52, 527–539.
- Sun, Q., & Yang, L. (2003). The adsorption of basic dyes from aqueous solution on modified peat-resin particle. *Water Research*, 37, 1535–1544.
- Treybal, R.E., 1968. Mass transfer operations. Second ed., McGraw Hill, New York.
- Vinke, P., Van der Eijk, M., Verbree, M., Voskamp, A. F., & Van Bekkum, H. (1994). Modification of the surfaces of a gas activated carbon and chemically activated carbon with nitric acid, hydrochloric and ammonia. *Carbon*, 32, 675.
- Zhang, J., Li, Y., Zhang, C., & Jing, Y. (2008). Adsorption of malachite green from aqueous solution onto carbon prepared from *Arundo donax* root. *Journal of Hazardous Materials*, 150, 774–782.
- Zheng, Y., Zhu, Y. F., Wang, F., & Wang, A. (2015). Gelatin-grafted granular composite hydrogel for selective removal of malachite green. *Water, Air, and Soil Pollution*, 226, 354.